ELSEVIER

Water Research 39 (2005) 4969–4978

WATER RESEARCH

www.elsevier.com/locate/watres

Optimizing experimental design to estimate ammonia and nitrite oxidation biokinetic parameters from batch respirograms

Kartik Chandran[a,*], Barth F. Smets[b]

[a]*Earth and Environmental Engineering, Columbia University, New York, NY, USA*
[b]*Environment & Resources DTU, Technical University of Denmark, Lyngby, Denmark*

Received 11 February 2003; received in revised form 21 April 2005; accepted 5 October 2005

Abstract

Knowledge of relative NH_4^+–N to NO_2^-–N oxidation and NO_2^-–N to NO_3^-–N oxidation dynamics is essential before application of either single-step or two-step nitrification models to fit batch nitrification respirograms. We have previously shown that two step nitrification models based on respirometry permit the estimation of kinetic parameters for both nitrification steps from a single respirogram associated with NH_4^+–N to NO_3^-–N oxidation. However, two-step model parameter estimates are meaningful only under circumstances when the respirograms contain sufficient kinetic information pertaining to both steps. In this study, we present an operationally amenable extant batch nitrification respirometric assay to engender maximal information content in the resulting respirograms with respect to both constituent nitrification steps. The developed design consists of an initial NH_4^+–N pulse to a nitrifying biomass sample followed by an additional NO_2^-–N pulse at an optimal time point, which can be rigorously determined by maximizing the value of the determinant of the Fisher information matrix, Det(F) or, alternatively, by visually identifying the point of NH_4^+–N depletion during the respirometric assay. The proposed design is applicable for accurate determination of the Monod kinetic parameter estimates for both nitrification steps from batch respirograms even when the pseudo-first order rate coefficients for the two nitrification steps are nearly equal; a condition under which standard NH_4^+–N to NO_3^-–N respirograms typically lack information with respect to NO_2^-–N oxidation.

Keywords: Optimal experimental design; Nitrification biokinetics; Extant respirometry

1. Introduction

The increasing stringency in permissible *total*-N (as opposed to only NH_4^+–N) effluent wastewater discharge limits, coupled with a diverse array of NH_4^+–N and NO_2^-–N oxidation inhibitors in influent wastewater, warrants a mechanistic description of both NH_4^+–N and NO_2^-–N oxidation kinetics and inhibition for adequate design and control of biological nitrogen removal reactors. Traditional single-step modeling of nitrification is adequate under sole rate limitation by NH_4^+–N to NO_2^-–N oxidation (Chandran and Smets, 2000b). However, such modeling yields meaningless kinetic parameter estimates when NO_2^-–N to NO_3^-–N oxidation or both oxidation steps limit overall nitrification during periods of the test assay (Chandran and Smets, 2000b).

*Corresponding author. Columbia University, 918 S. W. Mudd, New York, NY 10027, USA. Tel.: +1 212 854 9027.
E-mail address: kc2288@columbia.edu (K. Chandran).

0043-1354/$ - see front matter © 2005 Elsevier Ltd. All rights reserved.
doi:10.1016/j.watres.2005.10.001

Nomenclature

NH_4^+–N	ammonium–nitrogen
NO_2^-–N	nitrite–nitrogen
NO_3^-–N	nitrate–nitrogen
NOD	nitrogenous oxygen demand
S_{NH}	NH_4^+–N concentration
S_{NO_2}	NO_2^-–N concentration
S_o	initial concentration
μ_{max}	maximum specific growth rate (t^{-1})
K_S	half saturation constant ($M\,L^{-3}$)
q	maximum specific substrate consumption rate ($M\,M^{-1}\,t^{-1}$)
k	pseudo first order rate coefficient ($M\,M^{-1}\,t^{-1}$)
f_S	biomass yield coefficient ($M\,M^{-1}$)
ρ	parameter correlation coefficient
F	Fisher information matrix
Det(F)	determinant of F
X	covariance matrix
$x_{i,j}$	element of covariance matrix in ith row and jth column
RMS	residual mean square
SE_i	standard error associated with ith parameter
y	vector of model predictions at time t_j ($j = 1$ to N); (in this case: DO concentrations)
Q	vector containing weighting coefficients (each set to unity in this work)
θ	vector of model parameter ($i = 1$ to P, in this case 4)
SSE	sum of squared errors between measured and simulated state variables (in this case DO concentrations) ($M^2\,L^{-6}$)
$N-P$	(Eq. (8)) degrees of freedom for parameter estimation, which is the difference between number of data points (N) and number of parameters estimated (P)
Subscripts	
ns	NH_4^+–N to NO_2^-–N oxidation
nb	NO_2^-–N to NO_3^-–N oxidation

On the other hand, (for e.g., rate-limitation of overall nitrification by NH_4^+–N and NO_2^-–N oxidation rather than sole rate-limitation by NH_4^+–N oxidation), respirometry-based two step nitrification models can permit biokinetic estimation of both NH_4^+–N to NO_2^-–N oxidation and NO_2^-–N to NO_3^-–N oxidation from a single NH_4^+–N to NO_3^-–N oxidation respirogram (Chandran and Smets, 2000a). Thus, for any nitrification design or control endeavors based on batch respirometry derived biokinetic estimates, it is beneficial to identify the rate-limiting step in overall nitrification by estimating and comparing the kinetics of each step. Such identification is possible by metabolically uncoupling the two steps via selective inhibition of NO_2^-–N oxidation and explicitly quantifying each nitrification step via two separate batch respirometric assays (Chandran and Smets, 2000b). Alternatively, it may be possible to maximize the information content of the NH_4^+–N to NO_3^-–N oxidation respirogram with respect to both nitrification steps, thereby facilitating the accurate biokinetic estimation of both nitrification steps from a single batch respirometric assay.

The primary objectives of this study were focused on the second approach:

> *To optimize a batch respirometric assay associated with* NH_4^+–N to NO_3^-–N *oxidation for maximal information content with respect to both constituent nitrification steps, irrespective of the rate-limiting step. To formulate an operationally amenable system-independent optimal design for estimating the biokinetic parameters of both* NH_4^+–N to NO_2^-–N *and* NO_2^-–N to NO_3^-–N *oxidation that does not require a priori knowledge of biokinetic parameter estimates of the steps.*

2. Materials and methods

2.1. Cultivation of a nitrifying enrichment culture

A nitrifying enrichment consortium was grown and maintained in a 10 L continuous reactor with an internal settling chamber, operated at an HRT of 1 d and a target SRT of 20 d. Details of reactor operation have been described previously (Chandran and Smets, 2000b). Upon attainment of steady state, mixed liquor was periodically withdrawn from the reactor and used in respirometric tests.

2.2. Extant respirometric assay for monitoring nitrification activity

The kinetics of NH_4^+–N and NO_2^-–N oxidation were measured via extant respirometry (Chandran and Smets, 2000b; Ellis et al., 1996). Biomass samples were withdrawn from the parent nitrifying reactor and amended with MOPS buffer at 20 mM for providing sufficient buffering to offset acidification caused by NH_4^+–N oxidation. Biomass samples were saturated with pure oxygen prior to the initiation of the respirometric assays. Parallel respirometric assays were performed at 25 °C in

two 40 ml glass vessels according to a previously detailed procedure (Chandran and Smets, 2000b).

2.3. Reagent solutions

Substrate stock solutions were freshly prepared prior to each set of respirometric assays using laboratory grade ammonium sulfate ($(NH_4)_2SO_4$, Fisher Scientific Co., NJ) and sodium nitrite ($NaNO_2$, Sigma Chemical Co., MO). In select experiments, sodium azide (NaN_3, Fisher Scientific Co.) was used to selectively inhibit NO_2^-–N to NO_3^-–N oxidation per (Chandran and Smets, 2000b).

2.4. Convention for expressing state variables

We follow a previously introduced convention to track state variables during respirometric nitrification assays by expressing reduced nitrogen species concentrations in terms of the nitrogenous oxygen demand (NOD), computed with respect to an appropriate reference nitrogen species (Chandran and Smets, 2001).

2.5. Determination of biomass concentrations

Biomass concentrations were measured as total chemical oxygen demand (tCOD) using commercially available reagents (Hach Chemical Co., Loveland, CO). Since the influent was devoid of soluble COD, the NH_4^+–N oxidizing biomass and NO_2^-–N oxidizing biomass concentrations are proportional to their respective biomass yield coefficients (Chandran and Smets, 2000b).

2.6. Kinetic models for NH_4^+–N and NO_2^-–N oxidation

The differential equations representing nitrogen removal, oxygen uptake and biomass synthesis have been derived earlier and are summarized here in a matrix format (Table 1) (Chandran, 1999). Differential equations for each species can be obtained by multiplying the kinetic terms in the last column of Table 1 with the appropriate stochiometric term in columns two through five.

2.7. Simulation-based optimization of initial NH_4^+–N and NO_2^-–N concentrations

A preliminary estimate of optimal initial NH_4^+–N ($S_{NH,o}$) and NO_2^-–N ($S_{NO_2,o}$) concentrations for extant respirometric assays describing NH_4^+–N to NO_2^-–N oxidation and NO_2^-–N to NO_3^-–N oxidation, respectively, was determined from simulations. The simulations were performed at different S_o values using previously reported parameter estimates (Chandran and Smets, 2000b) and incorporated random experimental noise coincident with instrument accuracy specifications provided by the manufacturer of the dissolved oxygen electrode (YSI model 5331, YSI Instruments, Yellow Springs, OH, normally distributed with $\mu = 0\,mg\,O_2/L$, $\sigma = 0.05\,mg\,O_2/L$). The simulations were fit to mathematical models describing NH_4^+–N to NO_2^-–N oxidation and NO_2^-–N to NO_3^-–N oxidation (Table 1), which do not contain terms for experimental noise, to determine q_{max} and K_S estimates for each S_o value. Briefly, the differential equations linking biomass growth, substrate consumption and oxygen uptake were

Table 1
Elements of the two-step nitrification model

State variable	S_{NH}	S_{NO_2}	Ou_{ns}	Ou_{nb}	X_{ns}	X_{nb}	
ns	$-\frac{(1+(0.3\times f_{S,ns}))}{f_{S,ns}}$	$+\frac{1}{3\times f_{S,ns}}$	$+\frac{(1-f_{S,ns})}{f_{S,ns}}$		$+1$		$\mu_{max,ns}\frac{X_{ns}S_{nh}}{K_{S,ns}+S_{nh}}$
nb		$-\frac{1}{f_{S,nb}}$		$+\frac{(1-f_{S,nb})}{f_{S,nb}}$		$+1$	$\mu_{max,nb}\frac{X_{nb}S_{NO_2}}{K_{S,nb}+S_{NO_2}}$

Note:
S_{NH} NH_4^+–N concentration (mg NOD L^{-1}).
X_{ns} NH_4^+–N oxidizing biomass concentration (mg COD L^{-1}).
$\mu_{max,ns}$ maximum specific growth rate for NH_4^+–N to NO_2^-–N oxidation (h^{-1}).
$K_{S,ns}$ half-saturation coefficient for NH_4^+–N to NO_2^-–N oxidation (mg NOD L^{-1}).
$f_{S,ns}$ biomass yield coefficient for NH_4^+–N to NO_2^-–N oxidation (mg × COD/mg NH_4^+–NOD oxidized to NO_2^-–N).
Ou_{ns} oxygen uptake accompanying NH_4^+–N to NO_2^-–N oxidation (mg O_2 L^{-1}).
S_{NO_2} NO_2^-–N concentration (mg NOD L^{-1}).
X_{nb} NO_2^-–N oxidizing biomass concentration (mg COD L^{-1}).
$\mu_{max,nb}$ maximum specific growth rate for NO_2^-–N to NO_3^-–N oxidation (h^{-1}).
$K_{S,nb}$ half-saturation coefficient for NO_2^-–N to NO_3^-–N oxidation (mg NOD L^{-1}).
$f_{S,nb}$ biomass yield coefficient for NO_2^-–N to NO_3^-–N oxidation (mg × COD/mg NO_2^-–NOD oxidized to NO_3^-–N).
Ou_{nb} oxygen uptake accompanying oxidation of NO_2^-–N to NO_3^-–N (mg O_2 L^{-1}).

simultaneously solved using a fourth-order Runge–Kutta method. The biokinetic parameters describing the appropriate nitrogen oxidation step, μ_{max} and K_S, were estimated by minimizing the sum of the squared errors (SSE) with respect to the experimental oxygen uptake profiles using the SOLVER® utility in MS Excel®. The maximum specific NH_4^+–N and NO_2^-–N oxidation activities were expressed in terms of the maximum specific substrate consumption rates (q_{max}) rather than specific growth rates (μ_{max}) since q_{max} is less sensitive than μ_{max} to possible variability in the biomass yield coefficient, f_S, which was also estimated from the batch nitrification respirograms (Chandran and Smets, 2001). The relationship between μ_{max} and q_{max} for NH_4^+–N to NO_2^-–N oxidation and NO_2^-–N to NO_3^-–N oxidation is summarized in Eqs. (1) and (2), respectively, which are derived from an electron balanced scheme for the two nitrification steps (Chandran and Smets, 2000b, 2001)

$$q_{max,ns} = \mu_{max,ns}\frac{(1+(0.3\times f_{S,ns}))}{f_{S,ns}}, \quad (1)$$

$$q_{max,nb} = \frac{\mu_{max,nb}}{f_{S,nb}}. \quad (2)$$

The optimal initial substrate concentration was defined at the minimum beyond which values of a pseudo-first-order coefficient, k ($k = q_{max}X_o/K_S$) were relatively constant. Previous works have identified parameter combinations, which are structurally identifiable from respirometric data, not corrupted by experimental noise (Dochain et al., 1995; Petersen et al., 2003; Sperandio and Paul, 2000). On the other hand, the presence of noise in experimental data and limitations to numerical parameter estimation algorithms that process such data can result in poor practical parameter identifiability, leading to several parameter combinations resulting in equally good best-fit profiles (Holmberg, 1982; Marsili-Libelli, 1992; Vanrolleghem et al., 1995). For Monod-based functions, practical identifiability of μ_{max} (or alternately, q_{max}) and K_S depends upon the initial substrate concentration, noise level and sampling time points (Holmberg, 1982; Vanrolleghem et al., 1995). Therefore, rather than using q_{max} and K_S estimates, which can be highly correlated (as depicted in the results herein as well), we used k to draw inferences on S_o.

2.8. Experimental optimization of initial NH_4^+–N and NO_2^-–N concentrations

Following simulation-based determination, the optimum $S_{NH,o}$ and $S_{NO_2,o}$ values were subsequently experimentally determined from batch respirometric assays describing NH_4^+–N to NO_2^-–N oxidation and NO_2^-–N to NO_3^-–N oxidation, respectively. Extant respirometric assays were conducted at different initial NH_4^+–N and NO_2^-–N concentrations in the range 4.5–25 mg NH_4^+–NOD/L and 1.5–15 mg NO_2^-–NOD/L, respectively. The optimum initial NH_4^+–N and NO_2^-–N concentrations were the minimum NH_4^+–N and NO_2^-–N concentrations at which the running slope ($n = 6$–7, corresponding to three S_o concentrations) of the k vs. S_o profile was closest to zero, indicating that k was no longer impacted by S_o.

2.9. Kinetics of NH_4^+–N and NO_2^-–N oxidation from isolated respirometric assays

The kinetics of NH_4^+–N to NO_2^-–N oxidation were determined from a respirogram obtained in response to a NH_4^+–N pulse, with selective inhibition of NO_2^-–N to NO_3^-–N using 24 mM NaN_3 (Chandran, 1999; Ginestet et al., 1998). The kinetics of NO_2^-–N to NO_3^-–N oxidation were obtained from a respirogram in response to a NO_2^-–N pulse. These assays in which the two nitrification steps were explicitly quantified are termed *isolated* assays. Kinetic parameter estimates for each nitrification step were determined by fitting the biokinetic expressions for NH_4^+–N to NO_2^-–N oxidation (Table 1, row 2, denoted by ns) or NO_2^-–N to NO_3^-–N oxidation (Table 1, row 3, denoted by nb) to respirograms from the isolated NH_4^+–N oxidation or NO_2^-–N oxidation assays.

2.10. Kinetics of NH_4^+–N and NO_2^-–N oxidation obtained using the two-step nitrification model

In addition, respirograms were also obtained that represented NH_4^+–N to NO_3^-–N oxidation from *complete* respirometric assays conducted at the optimal $S_{NH,o}$ determined above. In select experiments, the initial NH_4^+–N pulse was followed by an NO_2^-–N pulse, also at the optimal initial concentration determined above (see section below on Optimal experimental design for biokinetic estimation of nitrification). Kinetic parameter estimates for each nitrification step were estimated by fitting the *complete* respirograms to the two step model (Table 1, rows 2 and 3).

2.11. Accuracy of two-step model parameter estimates

The kinetic parameter estimates obtained by fitting the two-step nitrification model to *complete* respirograms were compared with those obtained by fitting the model describing each nitrification step to *isolated* respirograms. Due to practical identifiability limitations of q_{max} and K_S in Monod-type functions, mentioned above, the accuracy of the two-step model parameter estimates was determined by comparing the pseudo first-order coefficient, k, obtained from the *complete* and *isolated* assays, for the different designs considered.

2.12. Optimal experimental design for biokinetic estimation of nitrification

Optimal experimental design for biokinetic estimation of nitrification was based on following an initial NH_4^+–N pulse to the test nitrification biomass with a subsequent NO_2^-–N pulse at an optimally determined t_{pulse} value, in order to increase the information content of the nitrification respirogram with respect to NO_2^-–N to NO_3^-–N oxidation. Briefly, as we have demonstrated previously (Chandran and Smets, 2000a), *complete* nitrification respirograms describing NH_4^+–N to NO_3^-–N oxidation lack information pertaining to the biokinetics of the second nitrification step, NO_2^-–N to NO_3^-–N oxidation, when the first nitrification step, NH_4^+–N to NO_2^-–N oxidation is the sole rate determining step. Indeed, under progressively higher overall rate limitation by NO_2^-–N to NO_3^-–N oxidation, the information content of *complete* nitrification respirograms is increasingly enriched with respect to this step (Chandran and Smets, 2000a). Recognizing that the rate determining step in nitrification may not always be known a priori, the information content on NO_2^-–N to NO_3^-–N oxidation might also be increased by providing a region in the respirogram, which is experimentally weighted towards NO_2^-–N oxidation. Therefore, we seek to enrich the information content of *complete* nitrification respirograms by following the initial NH_4^+–N pulse with an additional NO_2^-–N pulse.

Bioassay optimization and parameter identifiability calculations were based on the computation of the Fisher information matrix, F, which is a measure of the information content of experimental data (Bates and Watts, 1988). The optimal t_{pulse} value, which corresponded to the maximum practical identifiability in parameters of NH_4^+–N and NO_2^-–N oxidation was determined by maximizing the value of the determinant of F, Det(F), computed based on two-step model best-fit parameter estimates, as previously described (Chandran and Smets, 2000a) at each simulated t_{pulse}.

The Fisher information matrix (F) expresses the information content of experimental data and equals (Ljung, 1987):

$$F = \sum_{j=1}^{N} \left(\frac{\partial y}{\partial \theta_i}(t_j)\right)^{T} Q_j \left(\frac{\partial y}{\partial \theta_i}(t_j)\right). \tag{3}$$

Q was considered to be an identity matrix since only one state variable was measured (oxygen uptake) and the measurement errors were assumed to be constant over time. Therefore, the Fisher information matrix a $P \times P$ matrix with diagonal elements of the form:

$$f_{i,i} = \sum_{j=1}^{N} \left(\frac{\partial y}{\partial \theta_i}(t_j)\right)^{2} \tag{4}$$

and off-diagonal elements of the form:

$$f_{i,k} = \sum_{j=1}^{N} \left(\frac{\partial y}{\partial \theta_i}(t_j)\right)\left(\frac{\partial y}{\partial \theta_k}(t_j)\right). \tag{5}$$

To calculate the elements of F for a given experimental data set, a numerical respirometric profile was generated with one of the four two-step model parameters perturbed a small distance ($\delta\theta_i$, typically 1%) from its optimum estimate, keeping all other parameters at their respective optima. The difference between the respirogram thus obtained and the best-fit respirogram was evaluated at each time point (t_j) to give:

$$\frac{\partial y}{\partial \theta}(t_j) \approx \frac{\Delta y}{\Delta \theta_i}(t_j). \tag{6}$$

This procedure was repeated with small perturbations for all other parameters and the resulting F was calculated with Eqs. (4) and (5). Linearity of the SSE function in the region of perturbation was confirmed by the equality of $\sum_{j=1}^{N}(\partial y/\partial\theta)(t_j)$ on either side of the optimal parameter estimate.

Correlation between parameters of the single-step or two-step nitrification models was inferred from the correlation coefficients ρ_{ik} from the covariance matrix (X), which is the inverse of F (Robinson, 1985):

$$\rho_{i,k} = \frac{x_{i,k}}{(x_{i,i}x_{k,k})^{0.5}}, \tag{7}$$

where $x_{i,k}$ is the value of the element of the matrix X on row i and column k.

The precision of the ith kinetic parameter estimate of the two-step model was determined by calculating its standard error (Robinson, 1985).

$$\mathrm{RMS} = \frac{\mathrm{SSE}}{\mathrm{N} - \mathrm{P}}, \tag{8}$$

$$\mathrm{SE}_i = \sqrt{\mathrm{RMS}x_{i,i}}. \tag{9}$$

Numerically evaluated sensitivity coefficient profiles, $\theta_i(\partial y/\partial\theta_i)(t_j)$ were plotted for all parameters simultaneously to illustrate relative parameter sensitivities (Brouwer et al., 1998).

2.13. Preliminary simulations: rigorous determination of $t_{pulse,opt}$

Batch respirograms corresponding to NH_4^+–N to NO_3^-–N oxidation were simulated using a mechanistically derived two-step nitrification model (Chandran and Smets, 2000a), estimated values of biokinetic parameters (Chandran and Smets, 2000b) (Table 2, column 2) and representative random experimental noise. Simulated respirograms consisted of an initial 10 mg NH_4^+–NOD L^{-1} pulse followed by a 5 mg NO_2^-–NOD L^{-1} pulse at t_{pulse} values varying between 0.03 and 0.52 h after the time point of the NH_4^+–N

Table 2
Simulations indicating bias and correlation of best-fit parameter estimates to the two-step model

Parameters (units)	Simulation parameter value	Best-fit estimates	
		No pulse	Optimal $t_{pulse} = 0.47$ h
$q_{max,ns}$ (1/h)	0.12	0.14	0.12
$K_{S,ns}$ (mg NOD/L)	2	2.3	1.96
k_{ns} (1/h)	40.7	40.6	40.8
$q_{max,nb}$ (1/h)	0.2	0.07	0.2
$K_{S,nb}$ (mg NOD/L)	0.5	0.2	0.46
k_{nb} (1/h)	133.2	116.6	144.8
$\rho_{\mu_{max,ns}-K_{s,ns}}$		0.35	0.95
$\rho_{\mu_{max,ns}-\mu_{max,nb}}$		0	0.56
$\rho_{K_{s,ns}-K_{s,nb}}$		−0.54	0.38
$\rho_{\mu_{max,nb}-K_{s,nb}}$		0.6	0.96

Shaded rows depict significant decrease in bias for kinetic parameters of NO_2^-–N oxidation.
$S_{NH,o} = 10$ mg NH_4^+–NOD/L, $X_{ns,o} = 667$ mg COD/L; $X_{nb,o} = 333$ mg COD/L, $f_{S,ns} = 0.084$ mg × COD/mg NH_4^+–NOD, $f_{S,nb} = 0.1$ mg × COD/mg NO_2^-–NOD.

pulse. This rigorous approach to determine $t_{pulse,opt}$ via computation of Det(F), however, requires an a priori knowledge of the kinetic parameter estimates for NH_4^+–N and NO_2^-–N oxidation. Therefore, we explored possible system independent characteristics that could be used for optimizing nitrification respirometric assays for parameter estimation.

2.14. Preliminary simulations: system independent determination of $t_{pulse,opt}$

We considered optimization based on universally applicable factors such as identification of the time point that signals the end of NH_4^+–N oxidation in the oxygen uptake rate (OUR) profile. Different end-points in time for NH_4^+–N to NO_3^-–N oxidation were simulated using different initial NH_4^+–N concentrations ($S_{NH,o} = 5$, 10, 15 mg NH_4^+–NOD L^{-1}). The optimum t_{pulse} for each $S_{NH,o}$ was at the maximum value of Det(F). For each $S_{NH,o}$ tested, possible coincidence between $t_{pulse,opt}$ and the end point of NH_4^+–N oxidation was examined.

2.15. Experimental validation of system independent optimization

Pulse injections of NO_2^-–N ($S_{NO_2,o} = 5$ mg NO_2^-–NOD/L) were performed to the extant respirometric vessel at different time points before and after the time point of NH_4^+–N exhaustion ($S_{NH_4,o} = 10$ mg NO_2^-–NOD/L). The difference in time points between the NH_4^+–N and NO_2^-–N pulses was recorded. Kinetic parameter estimates for each nitrification step, obtained at each experimental design (t_{pulse}) considered were estimated by fitting the resulting respirograms to the two step model (Table 1, rows 2 and 3).

3. Results

3.1. Optimum initial NH_4^+–N and NO_2^-–N concentrations

From simulations using previously reported biokinetic parameter estimates for NH_4^+–N to NO_2^-–N oxidation and NO_2^-–N to NO_3^-–N oxidation, we determined optimum $S_{NH,o}$ and $S_{NO_2,o}$ values of 10 mg NH_4^+–NOD/L and 5 mg NO_2^-–NOD/L, respectively (data not shown). These simulations were intended to describe *isolated* NH_4^+–N and NO_2^-–N oxidation assays. From experimental *isolated* NH_4^+–N and NO_2^-–N oxidation assays conducted at $S_{NH,o}$ in the range 4.4–25 mg NH_4^+–NOD/L and $S_{NO_2,o}$ in the range 1.5–15 mg NO_2^-–N/L, optimum $S_{NH,o}$ and $S_{NO_2,o}$ values of 10 mg NH_4^+–NOD/L and 5 mg NO_2^-–N/L were determined (Fig. 1). Therefore, the simulation-based and experimental optimization of $S_{NH,o}$ and $S_{NO_2,o}$ yielded consistent results.

3.2. Improved accuracy and precision of nitrification biokinetic parameter estimates due to NO_2^-–N pulsing: results from simulations

In the absence of an additional NO_2^-–N pulse, there was considerable bias in parameter estimates for NO_2^-–N to NO_3^-–N oxidation describing the simulated respirograms, but not in parameter estimates for NH_4^+–N to NO_2^-–N oxidation (Table 2). Simultaneous NH_4^+–N and NO_2^-–N pulses at $t_{pulse} = 0$ h, still resulted in considerable bias in parameter estimates of NO_2^-–N

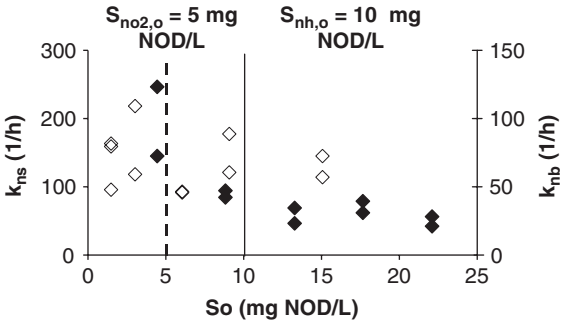

Fig. 1. Experimental optimization of $S_{NH,o}$ and $S_{NO_2,o}$ (◆: k_{ns}, ◇: k_{nb}). The solid and dashed vertical lines represent the optimum $S_{NH,o}$ and $S_{NO_2,o}$ values, respectively.

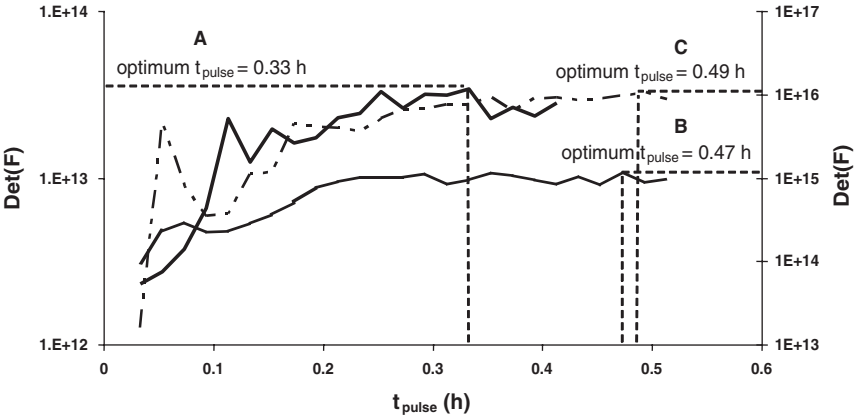

Fig. 2. Evolution of Det(F) for different t_{pulse} for different $S_{NH,o}$: (A) 5 mg NH_4^+–NOD/L (left-hand y-axis); (B) 10 mg NH_4^+–NOD/L (right-hand y-axis); (C) 15 mg NH_4^+–NOD/L (right-hand y-axis).

to NO_3^-–N oxidation (data not shown). For all t_{pulse} values in the range 0.03–0.52 h, parameter estimates describing NH_4^+–N to NO_2^-–N oxidation and NO_2^-–N oxidation were within 5% of the values used for simulating the batch respirograms (data not shown). Further, with increasing values of t_{pulse}, the value of Det(F) monotonically increased approximately 10-fold, irrespective of $S_{NH,o}$, till the point of NH_4^+–N exhaustion, indicating a significant improvement in the information content of the respirograms (Fig. 2). However, a relative plateau was observed in Det(F) beyond the region of NH_4^+–N exhaustion, visible especially for cases A and B (Fig. 2). For the optimal value of $S_{NH,o}$ at 10 mg NH_4^+–NOD/L, the optimal design corresponding to maximum Det(F) at t_{pulse} = 0.47 h (Fig. 3, Case B) resulted in accurate estimates for both nitrification steps (Table 2). The improvement in parameter accuracy of NO_2^-–N to NO_3^-–N oxidation was much more evident than the improvement in the accuracy of NH_4^+–N to NO_2^-–N oxidation parameters (Table 2). Parameter correlation *between* steps ($\rho_{\mu_{max,ns}-\mu_{max,nb}}\,\rho_{K_{s,ns}-K_{s,nb}}$) was significantly lower at the optimal design compared to parameter correlation *within* each step ($\rho_{\mu_{max,ns}-K_{s,ns}}\,\rho_{\mu_{max,nb}-K_{s,nb}}$) (Table 2, column 4). Uniformly high values of correlation coefficients ($\rho > 0.9$) *within* each step are attributed to low practical identifiability of parameters in the Monod model, estimated from extant respirometric assays (Chandran and Smets, 2000a; Vanrolleghem et al., 1995). A similar behavior in parameter correlation was observed for all designs considered (respirograms at different t_{pulse} values, data not shown).

3.3. System independent optimization based on end point of NH_4^+–N oxidation

From simulations, we observed that estimates of optimum t_{pulse} can be related to the time required for complete NH_4^+–N to NO_3^-–N oxidation (no NO_2^-–N pulse) (Fig. 3). The end point of NH_4^+–N to NO_3^-–N oxidation is clearly manifested in a sharp change in the OUR vs. time profile (Fig. 3) or a dissolved oxygen, DO, vs. time profile (Fig. 4) and may therefore be used as an experimentally applicable factor in determining $t_{pulse,opt}$.

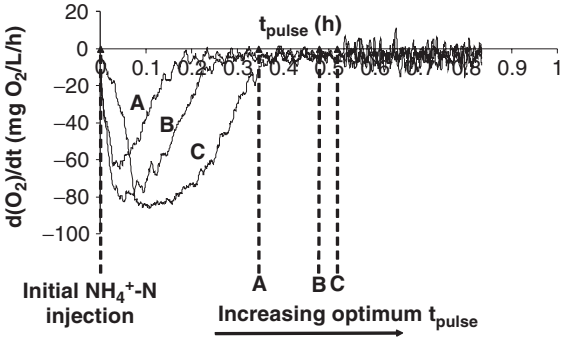

Fig. 3. Close correspondence of optimum t_{pulse} estimated at maximum Det(F); with the end point of NH_4^+–N to NO_3^-–N oxidation. Different end points were simulated using different initial NH_4^+–N concentrations: (A) 5 mg NH_4^+–NOD L^{-1}; (B) 10 mg NH_4^+–NOD L^{-1}; (C) 15 mg NH_4^+–NOD L^{-1}. Arrows correspond to rigorously determined $t_{pulse,opt}$ for simulations with 5 mg NH_4^+–NOD L^{-1} (A), 10 mg NH_4^+–NOD L^{-1} (B) and 15 mg NH_4^+–NOD L^{-1} (C).

3.4. Increased accuracy of two-step model parameter estimates by optimal design: experimental validation of system independent optimization

Improved accuracy of the parameter estimates was determined by comparing estimated two-step model pseudo first-order coefficients, k, from *complete* nitrification respirograms for different t_{pulse} values with

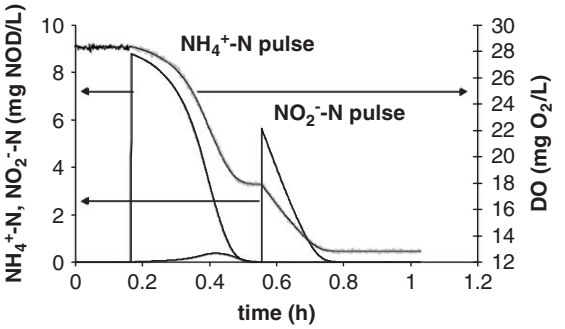

Fig. 4. Experimental (grey line) and modeled (black line) respirograms and NH_4^+–N and NO_2^-–N profiles based on a best fit respirogram for $t_{pulse} = 0.55$, or 0.39 h after the initial NH_4^+–N injection.

estimates obtained from *isolated* assays. In the absence of an NO_2^-–N pulse, considerable bias was observed in the two-step model parameter estimates from *complete* respirograms (Table 3, column 3) relative to estimates from *isolated* respirograms (Table 3, column 2). In the presence of an NO_2^-–N pulse, two-step model parameter estimates for both NH_4^+–N to NO_2^-–N oxidation and NO_2^-–N to NO_3^-–N oxidation were much closer to estimates from *isolated* assays (Table 3, columns 5–7) for t_{pulse} values in the vicinity of the optimal design (Table 3, cases 2–4). For sub-optimal designs (Table 3, cases 1 and 5), parameter accuracy was lower. Therefore, the optimal design reduced the bias in kinetic parameter estimates compared to sub-optimal designs. Further, the increase in accuracy of two-step nitrification model parameter estimates via the visual approximation of mathematically based optimal experimental design underlines the validity of this approximation.

3.5. Increased precision of two-step model parameter estimates by optimal design: experimental validation of system independent optimization

In the absence of an NO_2^-–N pulse, the poor information content of the resulting *complete* respirogram was reflected in the much lower Det(F) value associated with the best-fit parameters compared to those obtained with the added NO_2^-–N pulse (Table 3, row 5). For the NO_2^-–N pulse times considered, the average value of Det(F) was more than one order of magnitude higher for an NO_2^-–N pulse performed close to the point of complete NH_4^+–N oxidation (Table 3, cases 2–4), rather than during rapid NH_4^+–N oxidation (Table 3 high S_{NH}, case 1) or substantially after NH_4^+–N oxidation (Table 3, case 5). The average value of Det(F) and the information content of the batch respirograms was maximum when the additional NO_2^-–N pulse was

Table 3
Experimental validation of optimal t_{pulse}—variation of bias in estimates, Det(F), parameter correlation and standard error (SE) for best-fit two-step model parameter estimates from experimental respirograms, Avg±SD.

Case	Isolated assay	Complete assay	Complete assay with additional NO_2^-–N pulse			
			1	2	3	4	5
t_{pulse} (h)		None	0.25	0.33	0.36	0.39	0.61
k_{ns} (1/h)	71.36±8.19	144.8±47.8	22.29±8.23	66.07±17.81	87.7±11.05	60.5	54.65±7.18
k_{nb} (1/h)	71.88±23.02	59.1±23.3	56.08±28.52	70.91±5.93	62.04±11.96	70.4	55.04±6.08
Det(F)	ns: (1±0.95) 10^5 nb: (1.19±0.96) 10^4	2.75±2.82	$1 \times 10^{16} \pm 1.69 \times 10^{16}$	$3.6 \times 10^{17} \pm 2.73 \times 10^{16}$	$3.8 \times 10^{17} \pm 2.26 \times 10^{17}$	4×10^{17}	$1 \times 10^{16} \pm 1.36 \times 10^{14}$
$\rho_{\mu max,ns}-K_{s,ns}$	0.95±0.00	0.4±0.02	0.99±0.00	0.9±0.01	0.91±0.01	0.93	0.96±0.00
$\rho_{\mu max,ns}-\rho_{\mu max,nb}$	NA	−0.8±0.15	0.55±0.25	0.09±0.1	−0.01±0.04	−0.04	−0.23±0.01
$\rho_{K_s,ns}-K_{s,nb}$	NA	−0.12±0.37	0.27±0.49	−0.33±0.05	−0.35±0.01	−0.37	−0.46±0.00
$\rho_{\mu max,nb}-K_{s,nb}$	0.96±0.00	1±0.00	0.92±0.09	0.98±0.00	0.97±0.00	0.97	0.97±0.00
SE($\mu_{max,ns}$)	0.001±0.001	$4.95 \times 10^{-5} \pm 3.38 \times 10^{-5}$	$2.02 \times 10^{-4} \pm 1.76 \times 10^{-5}$	$2.84 \times 10^{-5} \pm 6.72 \times 10^{-6}$	$2.49 \times 10^{-5} \pm 4.05 \times 10^{-6}$	3.95×10^{-5}	$8.88 \times 10^{-5} \pm 1.04 \times 10^{-5}$
SE($K_{S,ns}$)	0.07±0.08	0.02±0.01	0.24±0.1	0.02±0.01	0.02±0.00	0.03±0.01	0.06±0.00
SE($\mu_{max,nb}$)	0.01±0.00	14.3±6.3	$5.65 \times 10^{-5} \pm 1.82 \times 10^{-5}$	$3.96 \times 10^{-5} \pm 7.22 \times 10^{-6}$	$3.9 \times 10^{-5} \pm 1.22 \times 10^{-5}$	2.98×10^{-5}	$4.26 \times 10^{-5} \pm 1.02 \times 10^{-5}$
SE($K_{S,nb}$)	0.03±0.01	2350±116	0.04±0.01	0.02±0.00	0.02±0.01	0.02	0.03±0.01
n	2	2	2	2	2	1	2

Shaded rows correspond to optimal t_{pulse} conditions.
Note: Single-step model was used for parameter estimation from the isolated assay respirograms.

performed between 0.33 and 0.39 h after the initial NH_4^+–N pulse (Table 3).

Further, in keeping with the simulation results, parameter correlation *within* each nitrification step was uniformly >0.9 for the different t_{pulse} values tested (Table 3). However, at the lowest and highest t_{pulse} considered, the magnitude of the correlation coefficients *between* the nitrification steps was significantly higher than that close to the point of NH_4^+–N exhaustion (Table 3). In addition, the superior quality of the parameter estimates in the region of the optimum t_{pulse} was evident from the lower corresponding parameter standard errors for Cases 2–4 compared to the parameter standard errors from the sub-optimal designs; Cases 1, 5 (Table 3). Further, in contrast to our simulation results, there was a decrease in information content and quality (decrease in Det(F), increase in parameter correlation coefficients, decrease in parameter precision) when the NO_2^-–N pulse was performed substantially after NH_4^+–N depletion (case 5), compared to injections close to NH_4^+–N exhaustion (cases 2–4). In general, the precision of parameters estimated from the *complete* optimally designed respirograms was higher, especially for μ_{max} estimates, than those estimated from *isolated* respirograms (Table 3).

4. Discussion

Step-wise quantification of nitrification kinetics via respirometry is possible by kinetic or metabolic uncoupling of NH_4^+–N to NO_2^-–N oxidation and NO_2^-–N to NO_3^-–N oxidation (Chandran and Smets, 2000b; Chudoba et al., 1985). Alternatively, explicit kinetic characterization of the two nitrification steps can be further simplified, if we recognize that the overall nitrification respirogram contains biokinetic information pertaining to both NH_4^+–N and NO_2^-–N oxidation.

When the rate of NH_4^+–N to NO_2^-–N oxidation is comparable to or lower than the rate of NO_2^-–N to NO_3^-–N oxidation, *complete* NH_4^+–N oxidation respirograms may not contain sufficient information pertaining to NO_2^-–N oxidation (Chandran and Smets, 2000a). Consequently, application of a two-step model nitrification model to describe such respirograms may result in high bias, high parameter correlation and low precision, of the estimated parameters, especially those for NO_2^-–N to NO_3^-–N oxidation (Table 2). We have previously shown that severe rate limitation by NO_2^-–N to NO_3^-–N oxidation ($k_{ns} > k_{nb}$), which may cause transient accumulation and persistence of NO_2^-–N even after NH_4^+–N depletion during a batch respirometric assay can significantly improve the information content of *complete* NH_4^+–N oxidation respirograms with respect to NO_2^-–N to NO_3^-–N oxidation (Chandran and Smets, 2000a). The dual rate-limitation of NH_4^+–N to NO_3^-–N oxidation by both NH_4^+–N to NO_2^-–N oxidation and NO_2^-–N to NO_3^-–N oxidation, in this study, is evident from the near equality of the pseudo-first-order rate coefficients of the two nitrification steps obtained from *isolated* assays (Table 3, column 2). Therefore, the poor parameter quality obtained by correlating the two-step nitrification model to *complete* nitrification respirograms is expected (Table 3, column 3).

The information content of experimental data can be enhanced by sampling more frequently or selectively during defined periods of the experiment or alternatively finding the input functions that lead to the most informative experiments (Munack, 1991; Robinson, 1985; Vanrolleghem et al., 1995). In this study, we increased the information content of a *complete* NH_4^+–N oxidation respirogram by following the initial NH_4^+–N pulse with a NO_2^-–N pulse.

Optimal experimental design for parameter estimation is a recursive process, since the design is dependent upon the parameter estimates itself and therefore, system specific (Petersen, 2000). The difference in the value of $t_{pulse,optimum}$ determined from the simulation-based and experimental respirograms highlights the strong dependence of the optimal design on the values of the governing biokinetic parameter estimates (Tables 2 and 3). Further, the parameters characterizing nitrification in continuously operated bioreactors may themselves vary with time due to transients in influent wastewater or reactor microbial population dynamics (Petersen, 2000; Vanrolleghem et al., 1995). Our simulations and experimental results reveal that rather than determining a specific $t_{pulse,opt}$ for a given kinetic parameter set, the NO_2^-–N pulse maybe performed close to the point of NH_4^+–N depletion and still adequately portray a more rigorously formulated optimal design. Since the point of NH_4^+–N depletion is manifested by a sharp change in curvature in DO vs. time (or OUR vs. time) profiles, this point can be chosen as the point of the NO_2^-–N pulse for an operationally amenable optimal experimental design. It is not surprising that $t_{pulse,opt}$ (corresponding to the maxima for det(F)) coincides with the point of NH_4^+–N depletion, since under this scenario, the information pertaining to NO_2^-–N to NO_3^-–N oxidation is separated from the region of concurrent NH_4^+–N and NO_2^-–N oxidation. The accompanying parameter identifiability analysis corroborates that such a combined respirogram contains adequate information pertaining to both steps (Tables 2 and 3). Therefore, there is a sound basis for choosing this approximation.

The presented optimal design involves a simple extension to a NH_4^+–N to NO_3^-–N respirometric assay and is therefore experimentally more favorable than performing two *isolated* respirometric assays via selective inhibition of NO_2^-–N to NO_3^-–N oxidation

(Chandran and Smets, 2000b). Further, the approach necessitates parameter estimation and identifiability of only one respirogram (for both oxidation steps) and is also more analytically favorable than via the selective inhibition approach (Chandran and Smets, 2000b). Therefore, the optimized nitrification assay maybe adapted for rapid routine monitoring of nitrification kinetics in continuously operated bioreactors.

5. Conclusions

In this study, we developed an optimal experimental design criterion to enable maximization of nitrification batch respirograms with respect to both NH_4^+–N to NO_2^-–N oxidation and NO_2^-–N to NO_3^-–N oxidation. Further, we present a simple extension to a conventional nitrification respirometric assay that significantly enhances the accuracy and precision of kinetic parameters describing both NH_4^+–N to NO_2^-–N oxidation and NO_2^-–N to NO_3^-–N oxidation from a single respirogram. The developed method involves following an initial NH_4^+–N pulse with an NO_2^-–N pulse at an optimally determined time point. The optimum time point can be rigorously determined based on the maximum value of the determinant of the Fisher information matrix associated with the parameter estimates. Alternatively, the optimum time point can be adequately approximated by visually identifying the point of NH_4^+–N depletion during the actual course of the batch respirometric assay.

Acknowledgements

This study was funded, in part, by the Connecticut Department of Environmental Protection through a US Environmental Protection Agency Long Island Sound Study grant under Section 119 of the Clean Water Act.

References

Bates, D.M., Watts, D.G., 1988. Nonlinear Regression Analysis and its Applications. Wiley, New York.

Brouwer, H., Klapwijk, A., Keesman, K.J., 1998. Identification of activated sludge and wastewater characteristics using respirometric batch-experiments. Water Res. 32, 1240–1254.

Chandran, K., 1999. Biokinetic characterization of ammonia and nitrite oxidation by a mixed nitrifying culture using extant respirometry. Thesis, University of Connecticut, CT. Summary at http://digitalcommons.uconn.edu/dissertations/AAI9926238/

Chandran, K., Smets, B.F., 2000a. Applicability of two-step models in estimating nitrification kinetics from batch respirograms under different relative dynamics of ammonia and nitrite oxidation. Biotechnol. Bioeng. 70, 54–64.

Chandran, K., Smets, B.F., 2000b. Single-step nitrification models erroneously describe batch ammonia oxidation profiles when nitrite oxidation becomes rate limiting. Biotechnol. Bioeng. 68, 396–406.

Chandran, K., Smets, B.F., 2001. Estimating biomass yield coefficients for autotrophic ammonia and nitrite oxidation from batch respirograms. Water Res. 35, 3153–3156.

Chudoba, J., Cech, J.S., Chudoba, P., 1985. The effects of aeration tank configuration on nitrification kinetics. J. Water Pollut. Control Fed. 57, 1078–1083.

Dochain, D., Vanrolleghem, A., van Daele, M., 1995. Structural identifiability of biokinetic models of activated sludge respiration. Water Res. 29, 2571–2578.

Ellis, T.G., Barbeau, D.S., Smets, B.F., Grady Jr., C.P.L., 1996. Respirometric technique for determination of extant kinetic parameters describing biodegradation. Water Environ. Res. 68, 917–926.

Ginestet, P., Audic, J.M., Urbain, V., Block, J.-C., 1998. Estimation of nitrifying bacterial activities by measuring oxygen uptake in the presence of the metabolic inhibitors allylthiourea and azide. Appl. Environ. Microbiol. 64, 2266–2268.

Holmberg, A., 1982. On the practical identifiability of microbial growth models incorporating Michaelis–Menten type nonlinearities. Math. Biosci. 62, 23–43.

Ljung, L., 1987. System Identification—Theory for the User. Prentice-Hall, Englewood Cliffs, NJ.

Marsili-Libelli, S., 1992. Parameter estimation of ecological models. Ecol. Model. 62, 233–258.

Munack, A., 1991. Optimization of sampling. In: Schugerl, K. (Ed.), Biotechnology, a Multi-Volume Comprehensive Treatise. VCH, Weinheim, Germany, pp. 251–264.

Petersen, B., 2000. Calibration, identifiability and optimal experimental design of activated sludge models. Thesis, Gent University, http://biomath.rug.ac.be/publications/download/petersenbritta_phd.pdf.

Petersen, B., Gernaey, K., Devisscher, M., Dochain, D., Vanrolleghem, P.A., 2003. A simplified method to assess structurally identifiable parameters in Monod-based activated sludge models. Water Res. 37, 2893–2904.

Robinson, J.A., 1985. Determining microbial kinetic parameters using nonlinear regression analysis. In: Marshall, K.C. (Ed.), Advances in Microbial Ecology. Plenum Press, New York, pp. 61–114.

Sperandio, M., Paul, E., 2000. Estimation of wastewater biodegradable COD fractions by combining respirometric experiments in various S_o/X_o ratios. Water Res. 34, 1233–1246.

Vanrolleghem, P.A., vanDaele, M., Dochain, D., 1995. Practical identifiability of a biokinetic model of activated sludge respiration. Water Res. 29, 2561–2570.